Dalton Transactions

Accepted Manuscript

ROYAL SOCIETY OF CHEMISTRY

www.rsc.org/dalton

TOC

Graphic abstract

Two one-dimensional coordination polymers with pentagonal bipyramidal Dy^{III} centres show slow magnetic relaxation featuring single molecule magnet behavior.

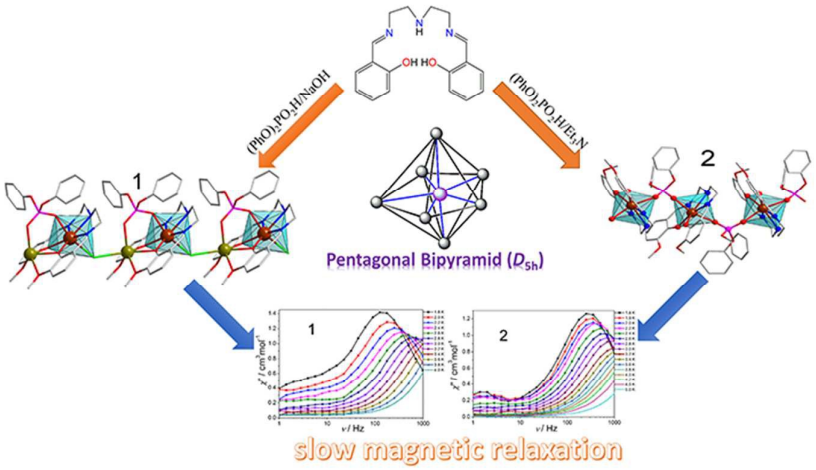

Journal Name

COMMUNICATION

Single Molecule Magnet Behavior Observed in 1-D Dysprosium Chain with quasi-D_{5h} Symmetry†

Received 00th January 20xx,
Accepted 00th January 20xx

DOI: 10.1039/x0xx00000x

www.rsc.org/

Xing-Cai Huang,[a,b] Ming Zhang,[a] Dayu Wu,*[a] Dong Shao,[b] Xin-Hua Zhao,[b] Wei Huang[a] and Xin-Yi Wang*[b]

Two one-dimensional (1-D) chain complexes with pentagonal bipyramidal Dy^{III} centers have been synthesized and magnetically characterized. Field-induced single molecule magnet behavior has been revealed in both compounds, which is still rarely reported in a lanthanide compound with a pentagonal bipyramid coordination geometry. Their crystal field parameters and orientations of the magnetic easy axes were obtained from the simulation of the magnetic data and the electrostatic model calculation.

Since the first discovery of the single-molecule magnet (SMM) behaviour of the sandwich complex $[N(C_4H_9)_4]^+[LnPc_2]^-$(Ln= Tb, Dy) in 2003,[1] mononuclear SMMs, commonly termed as single-ion magnets (SIMs), have been intensively studied because of their potential applications in molecular spintronics[2] and quantum-computing devices.[3] These mononuclear systems provide excellent models for understanding the magnetic anisotropy, i.e., especially single-ion anisotropy.[4] In lanthanide mononuclear SMMs, single-ion magnetic anisotropy depends on the competition between electrostatic crystal-field interaction and spin-orbit coupling.[5] The large unquenched orbital moment of lanthanides gives rise to their large magnetic anisotropy, making lanthanides good candidates for the construction of SMMs. To suppress the quantum tunnelling of magnetization frequently observed in the lanthanide SMMs, a ligand field of an axial symmetry, such as D_{4d}, D_{5h}, $D_{\infty h}$, S_8 (I_4), D_{6d} and so on, is usually preferred. For examples, the following SMMs contain lanthanides of approximate D_{4d} local symmetry: $[Pc'_2Ln]^{\pm/0}$,[6] $[Ln(W_5O_{18})_2]^{9-}$ (Ln = Ho, Er) and $[Ln(SiW_{11}O_{39})_2]^{13-}$ (Ln = Dy, Ho, Er, Yb),[7] lanthanide β-diketone,[8] and $[Ln(DOTA)(H_2O)]^-$ (Ln = Dy, Er, Yb) systems.[9] Organometallic double-decker lanthanide SMMs, (Cp*)Er(COT), $Ln(COT)^{2-}$(Ln = Er, Dy), and $[Ln(COT'')_2]^-$ (Ln = Er, Dy, Ce), have high rank rotation axes (C_∞, S_8, C_8 axis).[10] Recently, strong magnetic anisotropy and SMM behaviour were reported in the $Ln[N(SiMe_3)_2]_3$ (Ln = Er, Dy) and their related compounds with a C_{3v} symmetry.[11]

In this regard, lanthanide complexes with pentagonal bipyramid geometry (D_{5h}), especially for the Kramers Dy^{III} ($^6H_{15/2}$) and Er^{III} ($^4I_{15/2}$) ion, are rarely reported to behave as SMMs, such as Dy,[12] Er,[13] Dy_2,[14] Zn_2Dy[15] and Fe_2Dy[16] systems. In these systems, the pentagonal geometry of a five-fold axis played a predominant role in the suppression of the quantum tunnelling and results in the high energy barrier of 305 cm^{-1} (439 K) for ZnDyZn compound compared to the similar compounds of an octahedron geometry.[15] Also, an energy barrier of 319 cm^{-1} (459 K) is observed for the FeDyFe compound, which is the highest anisotropy barrier for a 3d-4f SMMs.[16] Previously, we adopted pentadentate ligand to successfully design the 3d SMMs with quasi-D_{5h} geometry.[17] As these ligands can occupy the five equatorial coordination sites, a pentagonal bipyramid geometry can be achieved if the axial positions are occupied by only two ligands. As an excellent pentadentate ligand, H_2valdien (N1, N3-bis(3-methoxysalicylidene)diethylenetriamine) was widely used; and a series of SMMs based on this ligand were obtained, including the Dy_2,[18] Dy_{12},[19] Co_2Dy_2,[20] and Ni_4Ln_2 (Ln = Tb, Dy and Ho) compounds.[21] But in these complexes, Dy^{III} centres mostly adopted an eight-coordinate ligand environment. To lower the coordination number, bulky anions with large steric effect are available for constructing seven-coordinate complexes to gain the pentagonal bipyramid geometry (D_{5h}).

Based on the above consideration, we successfully synthesized a series of one-dimensional Ln^{III} coordination polymers (experimental details in ESI†) by combining the pentadentate ligand valdien and a bulky anion diphenyl phosphate ($[(PhO)_2PO_2]^-$)(Scheme 1). Herein, we report the syntheses, crystal structures and magnetic properties of two 1D Dy compounds $[DyNa(valdien)((PhO)_2PO_2)Cl]_n$ (**1**) and $[Dy(valdien)((PhO)_2PO_2)]_n$ (**2**) in detail. As expected, the Dy^{III}

[a] Jiangsu Key Laboratory of Advanced Catalytic Materials and Technology, Collaborative Innovation Center of Advanced Catalysis & Green Manufacturing, School of Petrochemical Engineering, Changzhou University, Changzhou, Jiangsu 213164, China; E-mail: wudy@cczu.edu.cn.
[b] State Key Laboratory of Coordination Chemistry, Collaborative Innovation Center of Advanced Microstructures, School of Chemistry and Chemical Engineering, Nanjing University, Nanjing, 210093, China. E-mail: wangxy66@nju.edu.cn.

†Electronic Supplementary Information (ESI) available: Experimental details, X-ray crystallography data, XRD, additional magnetic measurements data. CCDC 1415417, 1415418, 1432155-1432157 and 1432220. For ESI and crystallographic data in CIF or other electronic format see DOI: 10.1039/x0xx00000x

center adopts pentagonal bipyramidal geometry. Filed-induced slow magnetic relaxation, characteristic of SMM behavior, was observed in both compounds.

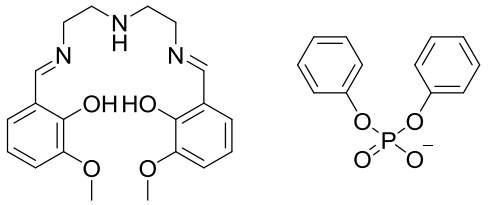

Scheme 1. The ligand **H_2valdien** and the bulky anion **$[(PhO)_2PO_2]^-$** as coligand.

Yellow block single crystals of compounds **1** and **2** were prepared by liquid diffusion of isopropyl ether into the mixture solution containing H_2valdien, Et_3N, $DyCl_3{\cdot}6H_2O$ and $(PhO)_2PO_2H$/NaOH or $(PhO)_2PO_2H/Et_3N$ (see the details including isostructural complexes **3**–**6** in ESI†). Single-crystal X-ray diffraction analyses revealed that compound **1** crystallizes in the orthorhombic space group *P*bca and compound **2** in the monoclinic space group $P2_1/c$ (Table S1, ESI†). Although both compounds are one-dimensional coordination polymers, the chains are different depending on the deprotonated bases used in the reaction: the chains in **1** are formed by the $[DyNa(valdien)((PhO)_2PO_2)]^-$ units bridged by the Cl^- anions; while the chains in **2** are formed by the $[Dy(valdien)]^+$ units bridged by the O-P-O group of the diphenyl phosphate (Fig. 1a and 1b). Every valdien ligand in **1** uses both its coordination pockets (N_3O_2 and O_4 pockets) to embrace both the Dy^{III} and Na^{I} ions, respectively; while for **2**, the O_4 pocket of the valdien ligand is empty. Interestingly, both Dy^{III} centres in compounds **1** and **2** are seven-coordinate with a distorted pentagonal bipyramid environment. The three nitrogen atoms and two oxygen atoms from the valdien ligands occupy the equatorial position of the Dy^{III} center, while the axial positions are occupied by one oxygen atom from the $[(PhO)_2PO_2)]^-$ ligand and one chloride anion in **1** and two oxygen atoms from two $[(PhO)_2PO_2)]^-$ ligands in **2** (Fig. 1c and 1d). As the pentagonal bipyramid geometry is distorted, the characteristic bond angels of the coordination geometry deviate from the ideal values for an ideal D_{5h} symmetry (Table S3, ESI†). The axial bond angles (O5–Dy1–Cl1 and O5–Dy1–O6) are 162.87(7) ° and 163.10(1) ° for **1** and **2**, respectively. Using the program SHAPE 2.1,[22] the continuous shape measures (CShM's) of the Dy^{III} centres relative to the ideal pentagonal bipyramid were calculated to be 0.775 and 0.496 for **1** and **2**, respectively (Table S4, ESI†). Separated by the anions and the bulky ligands, the Dy^{III} centres are isolated to each other: the shortest intra- and interchain $Dy^{III}\cdots Dy^{III}$ distances are of 8.3733(6) and 8.9941(5) Å for **1**, and 6.0538(8) 11.0268(5) Å for **2**, respectively (Fig. S2, ESI†), which fall in the range of the $Dy^{III}\cdots Dy^{III}$ distances in the reported 1D chain lanthanide SMMs.[23]

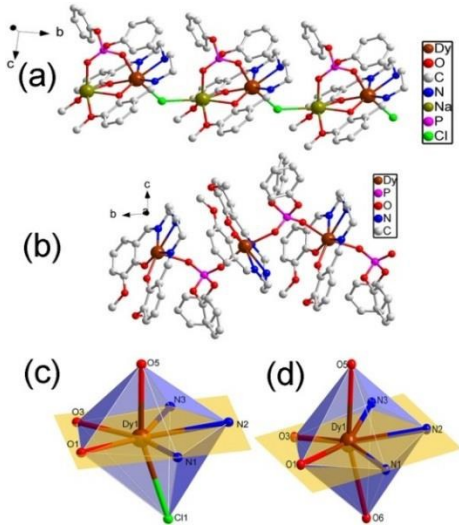

Fig. 1 The 1D chains of **1** (a) and **2** (b), and the coordination polyhedron around Dy^{III} centres with pentagonal bipyramid geometry (D_{5h}) for **1** (c) and **2** (d).

Direct-current (dc) magnetic susceptibilities of both **1** and **2** were performed on polycrystalline samples in the temperature range of 2.0–300 K under 1000 Oe (Fig. 2a and 2b). The $\chi_M T$ values at 300 K for **1** and **2** are 13.87 and 14.53 $cm^3mol^{-1}K$, respectively, which are close to the expected values (14.17 $cm^3mol^{-1}K$) for an isolated Dy^{III} ion (S = 5/2, L = 5, J = 15/2, $^6H_{15/2}$, g = 4/3). Upon cooling, the $\chi_M T$ values for **1** and **2** gradually decrease to 8.67 and 8.92 $cm^3\ mol^{-1}$ K at 2.0 K. This behaviour is mainly due to the thermal depopulation of the Dy^{III} Stark sublevels. The magnetization of both **1** and **2** at 2 K increases up to 5.26 and 5.56 μ_B at 70 kOe (Fig. 2a and 2b, inset), respectively, which is clearly lower than the expected saturation value for one uncorrelated Dy^{III} centre (10 μ_B), indicating the presence of magnetic anisotropy and/or low-lying excited states.

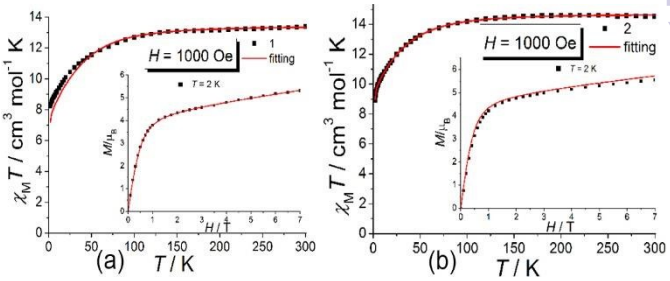

Fig. 2 χ_MT *vs*.T plots for **1** (a) and **2** (b) at 1000 Oe from 2–300 K and M *vs*. H plots for **1** and **2** at 2 K (inset), the red solid lines are fitted and simulated by the *PHI* program.

To understand the magnetic anisotropy on the Dy^{III} ion for both **1** and **2**, their magnetic susceptibility and magnetization data (Fig. 2a, b) were analysed simultaneously using the crystal field theory using the *PHI* program.[24] The Crystal-Field Hamiltonian is expressed in the Equation as following:

$$\widehat{H}_{\mathrm{CF}} = \sum_{i=1}^{N}\sum_{k=2,4,6}\sum_{q=-k}^{k}\sigma_i^k B_{k_i}^q \theta_k \hat{O}_{k_i}^q \qquad (1)$$

Where σ_i^k are the orbital reduction parameters, $B_{k_i}^q$ are the crystal field parameters (CFPs) in Steven's notation, θ_k are the

operator equivalent factors, and $\hat{O}_{k_i}^q$ are the operator equivalents. Considering the slightly distorted pentagonal bipyramid geometry of D_{5h} symmetry, only the parameters (B_2^0, B_4^0 and B_6^0) are adopted to avoid overparametrization.[15, 25] The CFPs (B_2^0, B_4^0 and B_6^0) and the anisotropy g-factors (g_x, g_y and g_z) were employed to fit the magnetic susceptibility and magnetization data. As can be seen in Figure 2, both the susceptibility and the magnetization data in the whole temperature range and up to the highest magnetic field can be fitted well with one set of parameters (Table S5, ESI†). With the obtained fitting parameters (CFPs and *g*-factors), the magnetic data of **1** and **2** are simulated to gain the energy-levels, the eigenstates and g-tensors. From the simulation of the ground state multiplet $^6H_{15/2}$ is given the energy-levels (listed in Table S6, ESI†), the energy gap between the ground state Kramers doublets (|m_J> = ±13/2) and the first excited states (|m_J> = ±11/2) are 41.63 cm^{-1} for **1** and 45.65 cm^{-1} for **2**, respectively. The local g-tensors on the ground doublets of the Dy sites show large g_z values, g_z= 15.46 for **1** and g_z= 17.44 for **2** (ideally g_x = g_y = 0, g_z = 20), indicating the easy axial magnetic anisotropy of both compounds.[23c, 26]

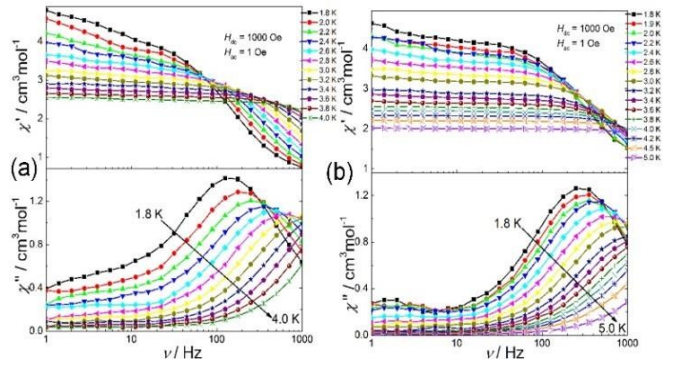

Fig. 3 Frequency dependence of the in-phase (χ′) and out-of-phase (χ″) ac susceptibility data under 1000 Oe dc field range from 1.8 to 4.0 K for **1** (a) and range from 1.8 to 5.0 K for **2** (b). The solid lines are a guide for the eye.

To probe the slow magnetic relaxation, the temperature and frequency-dependent ac susceptibilities were carried out in the temperature range of 1.8 –10 K for **1** and **2**. Under a zero dc field, no out-of-phase ac susceptibility (χ″) signal was observed above 1.8 K for both compounds, probably due to the fast QTM (Fig. S3 and S4, ESI†). However, to suppress the QTM effect, the 1000 Oe dc field was applied and both the in-phase (χ′) and out-of-phase (χ″) for **1** and **2** showed obvious temperature and frequency dependence (Fig. 3, Fig. S5 and S6, ESI†), indicating that the slow magnetic relaxation is originated from the single-ion magnetic behaviour of the Dy^{III} ion, as observed for other 1D or 2D Dy^{III} compounds with SMM behavior.[23]

The relaxation time (τ) can be obtained from the frequency-dependent ac susceptibility data (χ′ and χ″), and the corresponding Cole-Cole plots exhibit asymmetrically semi-circular shapes in the high frequency region and irregular curves in low frequency region, respectively (Fig. S7, ESI†). According to the generalized Debye model for the high frequency region,[27] the Cole–Cole plots at 1.8–4.0 K of **1** and at 1.8-5.0 K of **2** (Fig. S7, ESI†) can be fitted well, with α values in the range of 0.10–0.22 for **1** and 0.07–0.14 for **2** (Table S7 and S8, ESI†), respectively, indicating a relatively narrow distribution of the relaxation processes. To estimate the anisotropy energy barrier (U_{eff}), the high temperature data (Fig. 4) were fitted according to the Arrhenius law $\tau^{-1} = \tau_0^{-1} \exp(-U_{eff}/k_BT)$. The effective energy barrier U_{eff} were estimated to be 14.23 cm^{-1} (20.48 K) and 13.70 cm^{-1} (19.70 K) for **1** and **2**, respectively, with $\tau_0 = 2.56 \times 10^{-7}$ s for **1** and $\tau_0 = 6.12 \times 10^{-7}$ s for **2**. It is worthy to note that the plots of ln(τ) versus 1/*T* exhibit multiple relaxation processes under 1000 Oe field. In general, n = 9 for Kramers ions, smaller n values in the range of 1-6 can be considered as reasonable for an optical acoustic Raman process.[28] Considering the spin-lattice relaxation of both Raman and Orbach processes at low temperatures,[29] we could fit all the magnetic data with the equation (1) $\tau^{-1} = CT^n + \tau_0^{-1} \exp(-U_{eff}/k_BT)$, giving C =100.9 s^{-1}·K$^{-3.5}$, n=3.5, U_{eff} = 49.94 cm^{-1}, $\tau_0 = 1.50 \times 10^{-8}$ s for **1** and C =505.0 s^{-1}·K$^{-2.0}$, n=2.0, U_{eff} = 53.25 cm^{-1}, $\tau_0 = 3.03 \times 10^{-8}$ s for **2** (Fig. 4), which are close to the obtained energy gap from the the calculated values (*vide supra*). The results indicate that the Raman relaxation process could significantly influence the Orbach relaxation process on reducing the thermal energy barrier of the slow magnetic relaxation.[29a]

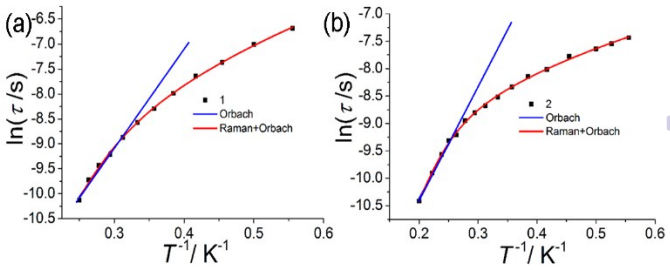

Fig. 4 The plots of ln(τ) versus 1/T at 1000 Oe dc field for **1**(a) and **2**(b). The blue and red solid lines represent the fitting by the Arrhenius law for high temperature region and for all the data, respectively.

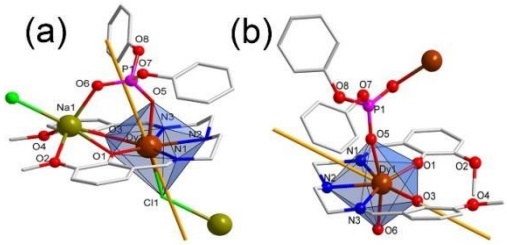

Fig. 5 The orientation of the magnetic easy axes (yellow) obtained according to an electrostatic model for **1** (a) and **2** (b).

To determine the magnetic anisotropy of the crystal field in both **1** and **2**, the orientation of the magnetic easy axes were estimated by an electrostatic model using the program *MAGELLAN* (Fig. 5a and 5b).[30] It is shown that the orientation of the magnetic easy axes in both **1** and **2** deviated remarkably from the pseudo-C5 axes of the pentagonal bipyramid geometry (D_{5h}) of Dy^{III} centres. This deviation is reasonable considering the fact that the pentagonal bipyramid of the Dy^{III} centres are distorted and there is no real 5-fold axis, not to

mention that the distribution of the negative charges has even lower symmetry. Also, the arrangement of magnetic axes could be related to the dynamic magnetic behavior in the both compounds.[31] This result emphasizes that one need to consider more on the negative charges of the coordination atoms for the rational design of lanthanide SMMs in specific symmetry.

In summary, these results demonstrate that the Dy^{III} compounds with pentagonal bipyramidal Dy^{III} centres can be rationally designed and synthesized. Due to the individual isolated system between the Dy^{III} ions, the two one dimensional Dy^{III} coordination polymers display single molecule magnet behavior with Raman process significantly affecting the Orbach relaxation process in this system. The fitting and simulating magnetic data in the crystal field parameters have been performed to gain insight into the possible mechanism of the slow magnetic relaxation. The method represents a potentially new design strategy leading toward the construction of a new class of SMMs. Future efforts will be devoted to the development of other heptacoordinate Dy(III) SMMs by controlling the single-ion anisotropy and/or the crystal field environment.

We thank the financial support by the Priority Academic Program Development of Jiangsu Higher Education Institutions (PAPD). This experiment work is financially funded by NSFC program (21371010, 21471023 & 21471077). Magnetic measurement was supported by SKLCC, Nanjing University.

Notes and references

1 N. Ishikawa, M. Sugita, T. Ishikawa, S. Koshihara and Y. Kaizu, *J. Am. Chem. Soc*., 2003, **125**, 8694.
2 (a) L. Bogani and W. Wernsdorfer, *Nat. Mater*., 2008, **7**, 179; (b) S. Sanvito, *Chem. Soc. Rev.,* 2011, **40**, 3336.
3 (a) M. N. Leuenberger, D. Loss, *Nature*, 2001, **410**, 789;(b) A. Ardavan, O. Rival, J. J. L. Morton, S. J. Blundell, A. M. Tyryshkin, G. A. Timco and R. E. P. Winpenny, *Phys. Rev. Lett.*, 2007, **98**, 057201.
4 S.-D. Jiang, B.-W. Wang and S. Gao, In *Molecular Nanomagnets and Related Phenomena*, *Struct. Bond*. , 2015, **164**, p 111.
5 (a) J. D. Rinehart and J. R. Long, *Chem. Sci*., 2011, **2**, 2078; (b) R. Skomski, *Simple Models of Magnetism*, Oxford University Press, Oxford, 2008.
6 D. N. Woodruff, R. E. P. Winpenny and R. A. Layfield, *Chem. Rev.,* 2013, **113**, 5110.
7 (a) M. A. AlDamen, J. M. Clemente-Juan, E. Coronado, C. Martí-Gastaldo and A. Gaita-Ariño., *J. Am. Chem. Soc.*, 2008, **130**, 8874; (b) M. A. AlDamen, S. Cardona-Serra, J. M. Clemente-Juan, E. Coronado, A. Gaita-Ariño, C. Martí-Gzastaldo, F. Luis and O. Montero, *Inorg. Chem.,* 2009, **48**, 3467.
8 S.-D. Jiang, B. -W. Wang, G. Su, Z.-M. Wang and S. Gao, *Angew. Chem. Int. Ed.,* 2010, **49**, 7448.
9 (a) P.-E. Car, M. Perfetti, M. Mannini, A. Favre, A. Caneschi and R. Sessoli, *Chem. Commun.,* 2011, **47**, 3751; (b) G. Cucinotta, M. Perfetti, J. Luzon, M. Etienne, P.-E. Car, A. Caneschi, G. Calvez, K. Bernot and R. Sessoli, *Angew. Chem. Int. Ed.,* 2012, **51**, 1606; (c) M.-E. Boulon, G. Cucinotta, J. Luzon, C. Degl'Innocenti, M. Perfetti, K. Bernot, G. Calvez, A. Caneschi and R. Sessoli, *Angew. Chem. Int. Ed.,* 2013, **52**, 350.
10 (a) S.-D. Jiang, B.-W. Wang, H.-L. Sun, Z.-M. Wang and S. Gao, *J. Am. Chem. Soc.,* 2011, **133**, 4730; (b) K. R. Meihaus and J. R. Long, *J. Am. Chem. Soc*., 2013, **135**, 17952; (c) L. Ungur, J. J. Le Roy, I. Korobkov, M. Murugesu and L. F. Chibotaru, *Angew. Chem. Int. Ed*., 2014, **53**, 4413; (d) J. J. Le Roy, I. Korobkov and M. Murugesu, *Chem. Commun.,* 2014, **50** , 1602; (e) J. J. Le Roy, I. Korobkov, J. E. Kim, E. J. Schelter and M. Murugesu, *Dalton Trans.,* 2014, **43** , 2737.
11 (a) P. Zhang, L. Zhang, C. Wang, S. Xue, S.-Y. Lin and J. Tang, *J. Am. Chem. Soc*., 2014, **136**, 4484; (b) A. J. Brown, D. Pinkowicz, M. R. Saber and K. R. Dunbar, *Angew. Chem. Int. Ed*., 2015, **54**, 5864.
12 (a) E. L. Gavey, Y. Beldjoudi, J. M. Rawson, T. C. Stamatatosa and M. Pilkington, *Chem. Commun.,* 2014, **50**, 3741; (b) M. Ren, S.-S. Bao, B.-W. Wang, R. A. S. Ferreira, L.-M. Zheng and L. D. Carlos, *Inorg. Chem. Front*., 2015, **2**, 558.
13 M. Ren, S.-S. Bao, R. A. S. Ferreira, L.-M. Zheng and L. D. Carlos, *Chem. Commun*., 2014, **50**, 7621.
14 Y.-N. Guo, G.-F. Xu, W. Wernsdorfer, L. Ungur, Y. Guo, J. Tang, H.-J. Zhang, L. F. Chibotaru and A. K. Powell, *J. Am. Chem. Soc.*, 2011, **133**, 11948.
15 J.-L. Liu, Y.-C. Chen, Y.-Z. Zheng, W.-Q. Lin, L. Ungur, W. Wernsdorfer, L. F. Chibotaru and M.-L. Tong, *Chem. Sci*., 2013, **4**, 3310.
16 J.-L. Liu, J.-Y. Wu, Y.-C. Chen, V. Mereacre, A. K. Powell, L. Ungur, L. F. Chibotaru, X.-M. Chen and M.-L. Tong, *Angew. Chem. Int. Ed.* 2014, **53**, 12966.
17 X.-C. Huang, C. Zhou, D. Shao and X.-Y. Wang, *Inorg. Chem*., 2014, **53**, 12671.
18 (a) J. Long, F. Habib, P.-H. Lin, I. Korobkov, G. Enright, L. Ungur, W. Wernsdorfer, L. F. Chibotaru and M. Murugesu, *J. Am. Chem. Soc.*, 2011, **133**, 5319; (b) F. Habib, P.-H. Lin, J. Long, I. Korobkov, W. Wernsdorfer and M. Murugesu, *J. Am. Chem. Soc*., 2011, **133**, 8830; (c) F. Habib, G. Brunet, V. Vieru, I. Korobkov, L. F. Chibotaru and M. Murugesu, *J. Am. Chem. Soc.*, 2013, **135**, 13242; (d) G.Brunet, F. Habib, I. Korobkov and M. Murugesu, *Inorg. Chem*., 2015, **54**, 6195.
19 L. Zhao, S. Xue and J. Tang, *Inorg. Chem*., 2012, **51**, 5994.
20 L. Zhao, J. Wu, S. Xue and J. Tang, *Chem. Asian J*., 2012, **7**, 2419.
21 L. Zhao, J. Wu, H. Ke and J. Tang, *Inorg. Chem*., 2014, **53**, 3519.
22 M. Llunell, D. Casanova, J. Cirera, P. Alemany and S. Alvarez, *SHAPE*, version 2.1; Universitat de Barcelona: Barcelona, Spain, 2013.
23 (a) D.-D. Yin, Q. Chen, Y.-S. Meng, H.-L. Sun, Y.-Q. Zhang and S. Gao, *Chem. Sci*., 2015, **6**, 3095. (b) L. Jia, Q. Chen, Y.-S. Meng, H.-L. Sun and S. Gao, *Chem. Commun.,* 2014, **50**, 6052; (c) Q. Chen, Y.-S. Meng, Y.-Q. Zhang, S.-D. Jiang, H.-L. Sun and S. Gao, *Chem. Commun.,* 2014, **50**, 10434; (d) J. Jung, F. Le Natur, O. Cador, F. Pointillart, G. Calvez, C. Daiguebonne, O. Guillou, T. Guizouarn, B. Le Guennic and K. Bernot, *Chem. Commun.,* 2014, **50**, 13346; (e) Y.-C. Hui, Y.-S. Meng, Z. Li, Q. Chen, H.-L. Sun, Y.-Q. Zhang and S. Gao, *CrystEngComm*, 2015, **17**, 5620; (f) T. Han, J.-D. Leng, Y.-S. Ding, Y. Wang, Z. Zheng and Y. -Z. Zheng, *Dalton Trans*., 2015, **44**, 13480.
24 N. F. Chilton, R. P. Anderson, L. D. Turner, A. Soncini and K. S. Murray, *J. Comput. Chem*., 2013, **34**, 1164.
25 (a) A. Lannes and D. Luneau, *Inorg. Chem.*, 2015, **54**, 6736; (b) Q.-W. Li, J.-L. Liu, J.-H. Jia, Y.-C. Chen, J. Liu, L.-F. Wang and M.-L. Tong, *Chem. Commun.,* 2015, **51**, 10291; (c) C.Görller-Walrand, K. Binnemans, K. A. Gschneidner and L. Eyring, *Handbook on the Physics and Chemistry of Rare Earths*, 1996, vol. 23, p 121.
26 S. Gómez-Coca, D. Aravena, R. Morales and E. Ruiz, *Coord. Chem. Rev*., 2015, **289–290**, 379.

27 K. S. Cole and R. H. Cole, *J. Chem. Phys*., 1941, **9**, 341.
28 (a) A. Singh and K. N. Shrivastava, *Phys. Status Solidi B*, 1979, **95**, 273; (b) K. N. Shrivastava, *Phys. Status Solidi B*, 1983, **117**, 437.
29 (a) S. Titos-Padilla, J. Ruiz, J. M. Herrera, E. K. Brechin, W. Wersndorfer, F. Lloret and E. Colacio, *Inorg. Chem.*, 2013, **52**, 9620; (b) W.-B. Sun, P.-F. Yan, S.-D. Jiang, B.-W. Wang, Y.-Q. Zhang, H.-F. Li, P. Chen, Z.-M. Wang and S. Gao, *Chem. Sci.*, 2015, doi: 10.1039/C5SC02986D.
30 N. F. Chilton, D. Collison, E. J. L. McInnes, R. E. P. Winpenny and A. Soncini, *Nat. Commun*., 2013, **4**, 2551.
31 K. H. Zangana, E. M. Pineda and R. E. P. Winpenny, *Dalton Trans*., 2015, **44**, 12522.